7

Assessment of Stress Corrosion Cracking on Pipeline Steels Weldments Used in the Petroleum Industry by Slow Strain Rate Tests

A. Contreras[1], M. Salazar[1], A. Albiter[1], R. Galván[2] and O. Vega[3]
[1]*Instituto Mexicano del Petróleo,*
[2]*Universidad Veracruzana,*
[3]*Centro de Investigación en Materiales Avanzados-CIMAV*
México

1. Introduction

The Stress Corrosion Cracking (SCC) is a local corrosion process which is characterized by the initiation and propagation of cracks. It takes place under the simultaneous action of sustained tensile stresses and specific corrosive environment on a susceptible material.
The formation of SCC occurs below the yield strength of the material and typically below the design stress and fatigue limit of an engineering structure. Since the first discovery of SCC on the exterior surface of a buried high pressure natural gas transmission pipeline in 1965 (Leis & Eiber, 1997), SCC has continued to make a significant contribution to the number of leaks and ruptures in pipelines.
Two forms of SCC can exist on buried steel pipelines (Beavers & Harle, 2001). The first discovered form of SCC propagates intergranularly and is associated with a concentrated alkaline electrolyte in contact with the steel surface, commonly called as high pH-SCC or classical SCC. A second form of SCC was discovered in Canada in the early 1980. This form of SCC propagates transgranularly and is associated with a dilute neutral pH electrolyte in contact with the steel surface, commonly called as low pH-SCC, non-classical, or near neutral pH-SCC. Currently, there are some mechanisms proposed to explain the SCC occurrence including the following: (1) a role for hydrogen in enhancing crack tip dissolution; (2) a possible synergistic growth by fatigue and corrosion.
For high pH-SCC it is observed that the mechanism involves anodic dissolution for crack initiation and propagation. In contrast, for low pH-SCC is associated with the dissolution of the crack tip and sides, accompanied by the ingress of hydrogen in the steel. Steels with high tensile strength are more susceptible to SCC. Cracks propagate as a result of anodic dissolution in front of their tip in SCC process, due to the embrittlement of their tip by hydrogen based mechanism. It was revealed that cracking behavior of pipeline steel in the soil environment depends of the cathodic protection applied. Applying different potentials levels the dominance of SCC process changes. At relatively low potential, the steel cracking is based primarily on the anodic dissolution mechanism. When the applied potential increases negatively, hydrogen is involved in the cracking process, resulting in a transgranular cracking mode (Liu *et* al, 2008).

SCC can occur in both gas and liquid pipelines but is more common and catastrophic in gas pipelines (Manfredi & Otegui, 2002). SCC is the most unexpected form of pipeline failure that can involve no metal loss and must not be confused with wall thinning rupture. SCC on pipelines begins with small cracks develop on the outside surface of the buried pipe. These cracks are initially not visible to the eye and are most commonly found in colonies, with all the cracks in the same direction, perpendicular to the stress applied.
This chapter describes the mechanical and environmental effects as well fracture characteristics on SCC susceptibility of steels used in the oil industry using slow strain rate tests (SSRT), which were carried out according to requirements of NACE TM-0198, ASTM G-129 and NACE TM-0177 standards (NACE TM-0198, 2004; ASTM G-129, 2006; NACE TM 0177, 2005). Some tests were supplemented by potentiodynamic polarization and hydrogen diffusion tests. SSRT were performed in samples which include the longitudinal and circumferential weld bead of pipeline steels. The weld beads were produced using the submerged arc welding (SAW) and shielded metal arc welding (SMAW) process.
The SCC susceptibility has been evaluated using the results of SSRT in air (as an inert environment), sour solution according to NACE TM 0177 (solution A from method A) and in some cases a simulated soil solution called NS4. The studies include the effect of pH, temperature, microstructure, effect of multiple welding repairs and mechanical properties. The steels studied are low carbon steels API X52, X60, X65 and X70.

2. Stress corrosion cracking phenomena

2.1 What is SCC and how is presented in pipelines?

SCC is the cracking of the steel as result of the combined effect of corrosive environment and tensile stresses on a susceptible material. SCC is a term used to describe service failures in engineering materials produced by environmentally induced crack propagation (Jones, 1992). The stress required to produce SCC can be residual, externally applied or operational.
SCC on pipelines begins when small cracks develop on the external surface of buried pipelines. These cracks initially are no visible, but when the time pass, this individual cracks may growth and forms colonies, and many of them join together to form longer cracks.
The SCC phenomenon has four stages:

1. Cracks nucleation.
2. Slow growth of cracks.
3. Coalescence of cracks.
4. Crack propagation and failure.

This process can take many years depending on the conditions of steel, environment and stresses.

2.2 The conditions for stress corrosion cracking

The studies performed indicate that SCC initiate as a result of the interaction of three conditions as is shown in Figure 1. All the three conditions are necessary to SCC occurs. If any of these three conditions can be mitigate or eliminate to a point where cracking will not occur, the SCC can be prevented.

2.3 Types of stress corrosion cracking

Generally, there are two types of SCC related with the pH. The pH is measured from the environment in contact with the pipe surface. The type involving high pH (greater than 9) is

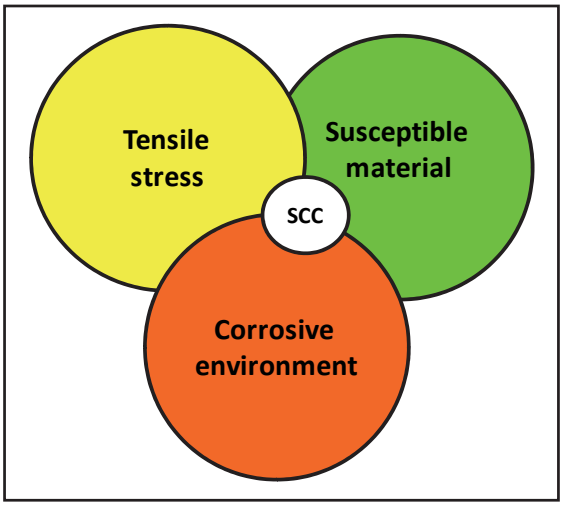

Fig. 1. Conditions necessary for SCC occur.

associated with intergranular cracking, while the type involving lower pH (<6) is associated mainly with transgranular cracking. High pH cracking generally involves rupture of passivating oxide films followed by dissolution in the crack tip (Krist & Leewis, 1998). Delanty *et* al. (Delanty & O'Beirne, 1992) found that the severity of the SCC increases with increasing bacterial concentration and the absence of oxygen.

High pH-SCC occurs only in a relatively narrow cathodic potential range (650-750 mV, $Cu/CuSO_4$) in presence of carbonate-bicarbonate environment and a pH greater than 9 (Stress Corrosion Cracking on Canadian Oil and Gas Pipelines, 1996). Growth cracks increases with temperature, and generally are cracks with no evidence of corrosion.

In contrast, it has been suggested that the low pH-SCC is associated with the dissolution of the crack tip and sides, accompanied by the ingress of hydrogen in the steel (Fang *et* al, 2003, 2010; Zhang *et* al, 1999). No apparent correlation with temperature was found; generally the pH range is between 5.5 to 7.5. A corrosion potential between 760 to 790 mV, $Cu/CuSO_4$ was observed, and wide cracks with evidence of corrosion. A comparative table of both SCC types was given elsewhere (Beavers & Harle, 2001).

2.4 Stress corrosion cracking evaluation techniques

2.4.1 Test methods

As was mentioned above to produce SCC in steel is necessary to apply tensile stresses on material susceptible exposed in a corrosive environment. To assess the SCC susceptibility there are many kinds of specimens including U-bends, bean beams, C-Ring and smooth tensile bars. More detail of these methods is given in NACE TM 0177.

The most common methods for testing these specimens are: 1) Constant Load Tests (CLT) using proof rings and 2) Constant Extension Rate Tests (CERT). The CLT gives few information due to only put the specimen in a specific solution for 30 days at tensile stress of 72% of yielding strength, if the specimen fail the steel no pass, if no fail the steel pass. The termination of the test shall be at tensile test specimen failure or after 720 hours, whichever occurs first.

The CERT method commonly is used with smooth tensile specimens through the SSRT. In these tests specimens are slowly strained in tension and simultaneously exposed to a corrosive environment. SCC susceptibility is evaluated by comparison of failure times, maximum stress, plastic elongation, strain or reduction in area to values obtained in tests conducted in an inert environment (Air). From this comparison of the mechanical properties mentioned above, a ratio is obtained. Additionally, scanning electron microscopy (SEM) observations of samples with low ratios (<0.8) should be carried out. More details of the evaluation of SCC susceptibility using SSRT is given on NACE TM-0198 and ASTM G-129.

2.4.2 Slow strain rate tests (SSRT)

In recent years the SSRT has become widely used and accepted for SCC evaluations to screen materials and to identify alloys that should not experience SCC in service. SSRT involves the slow straining of a specimen of the steel of interest in a solution in which will be in service. Typically a strain rate of the order of $1x10^{-6}$ in/sec is used, which is about four orders of magnitude slower than strain rate used in a standard tensile test. A major advantage of SSRT over CLT is that the test period is generally shorter. Thus, using SSRT we can screening or evaluate materials in a fast way within a few days to determine SCC susceptibility (Kane *et* al, 1997).

It is well known that the SSRT provides not only a useful information on SCC susceptibility of the materials in any corrosive environments, but also a relatively short experimental time to evaluate SCC susceptibility, where a maximum fracture time is that obtained at the lowest strain rate in an inert environment. For that reason, SSRT has been widely used for SCC assessment. However, to use SSRT for the SCC experiments, we need to compare the parameters (time to failure, maximum stress, strain, reduction area, plastic elongation, etc.) obtained in the corrosive environments with those in an inert environment. In addition, it must be kept in mind that the specimens are always fractured in both environments, by which in some cases it would be difficult to judge whether the fracture of the specimens takes place by SCC or not (Nishimura & Maeda, 2004).

2.5 Stress corrosion cracking assessment

The susceptibility to SCC is evaluated according to NACE TM-0177 for CLT, and according to NACE TM 0198 and ASTM G129 for SSR tests. To evaluate the SCC susceptibility through SSRT is expressed in terms of the percentage reduction in area (%RA) calculated by the following expression:

$$RA(\%) = \frac{(D_i^2 - D_f^2)x100}{D_i^2} \tag{1}$$

where D_f and D_i are the final and the initial diameters of the tensile specimen respectively. The reduction area ratio (RAR) after fracture for the specimen in the test environment (RA_e) to the corresponding value determined in the controlled environment (RA_c) was calculated according to the following expression:

$$RAR = \frac{RA_e}{RA_c} \tag{2}$$

Additionally, the SCC susceptibility using the time to failure ratio (TFR) can be evaluated according to the following equation:

$$TFR = \frac{TF_e}{TF_c} \tag{3}$$

where TF_e is the time to failure determined for the material in the test environment and TF_c is the time to failure to the corresponding value determined in the controlled environment. The similar way it can be assessed the SCC susceptibility using the plastic elongation according to the following expressions:

$$\%EP = \left[\frac{E_F}{L_I} - \left(\frac{\sigma_F}{\sigma_{PL}} \right) \left(\frac{E_{PL}}{L_I} \right) \right] x100 \tag{4}$$

$$EPR = \frac{EP_e}{EP_c} \tag{5}$$

where:
EP = Plastic strain to failure (%)
E_F = Elongation at failure (mm/in)
E_{PL} = Elongation at proportional limit (mm/in)
L_I = Initial gauge length (mm/in) (usually 25.4 mm/1 in)
σ_F = Stress at failure (MPa)
σ_{PL} = Stress at proportional limit (MPa)

Ratios in the range of 0.8-1.0 normally denote high resistance to environment assisted cracking (EAC), whereas low values (i.e.<0.5) show high susceptibility. Therefore, to maximize the SCC resistance, it is desirable to obtain values of ratios as close to unity as possible. Lower values of ratios generally indicate increasing susceptibility to SCC.
Complementary metallographic examination must be performed to establish whether or not there is SCC on the samples. Overalls when there is some uncertainty in the assessment of SCC susceptibility evaluating the mechanical properties (RAR, TFR, EPR). The presence of cracks must be evaluated on the longitudinal section of the gage. The SEM observation it is recommended when there is ratios lower than 0.8.

3. SCC susceptibility of low carbon steels

Pipelines of low carbon steel welded by electric arc have been used for many years and are widely used in the petroleum industry. However, frequent failures during operation over the years (Craig, 1998) have prompted several studies of the design, construction, operation and maintenance of equipment and metallic structures used in this industry. Oil and gas from Mexico contain entrained H_2O, CO_2 and H_2S mainly (Presage of production of the marine and south regions from México for a horizon of the 2000-2014). These constituents, when moving through the pipelines, induce failures, mainly in the weld bead. Studies of weld bead failures have demonstrated that these occur mainly in the heat affected zone (Greer, 1975). This is due to the heterogeneity in microstructure (grain growth) and residual stresses.

3.1 Materials

In this work the susceptibility to SCC and corrosion of the main pipeline steels used in the oil industry were investigated. API X52, X60, X65 and X70 pipeline steels were studied. The chemical compositions and equivalent carbon (C_{eq}) are showed in Table 1. Dimensions of the pipeline used in this study are showed in Table 2.

Steel	C	Mn	Si	P	S	Al	Nb	Ni	V	Mo	Ti	Cr	Cu	C_{eq}
X52-A	0.080	1.05	0.26	0.019	0.003	0.038	0.041	0.019	0.054	---	0.002	0.02	0.019	0.27
X52-B	0.090	0.89	0.30	0.006	0.0015	0.025	---	0.05	0.036	0.05	0.016	0.07	0.12	0.28
X60	0.020	1.57	0.14	0.013	0.002	0.046	0.095	0.17	0.004	0.05	0.014	0.26	0.30	0.32
X65	0.070	1.46	0.25	0.012	0.002	0.041	0.047	0.050	0.069	---	0.017	0.02	0.09	0.34
X70	0.027	1.51	0.13	0.014	0.002	0.035	0.093	0.16	0.004	0.004	0.011	0.27	0.28	0.36

Table 1. Chemical composition of the steels studied (wt.%).

Steel	Diameter (in)	Thickness (in)
X52-A X52-B	36 8	0.375 0.437
X60	42	0.500
X65	24	0.562
X70	36	0.902

Table 2. Dimensions of the pipeline studied.

The pipeline steels with longitudinal welding acquired in PMT (Productora Mexicana de Tubería) were used in this study. The longitudinal and circumferential welding were carried out by the technique of submerged arc welding (SAW) and shielded metal arc welding (SMAW).

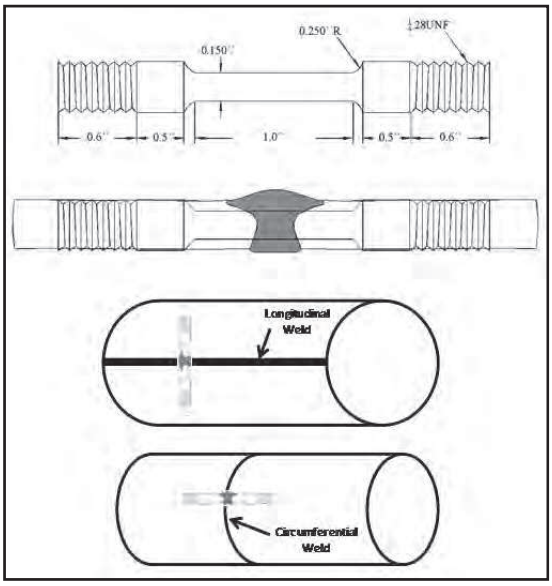

Fig. 2. Schematic representation where the specimens were obtained from the pipeline.

Cylindrical tensile specimens with a gauge length of 25.4 mm (1 inch) and 3.81 mm (0.150 inches) gauge diameter were machined from the pipeline perpendicular to weld bead as is shown in Figure 2.

3.2 Experimental set-up

To perform the SSR tests in the NACE solution saturated with H_2S and NS4 solution, a 500 mL glass autoclave as is shown in Figure 3(a) was used. The autoclave containing the specimen was externally heated by means of a heating element to the temperature required. A Solartron potentiostat controlled by a desktop computer was used for potentiodynamic polarization. The SSRT were performed in an Inter-Corr machine type M-CERT with load capacity of 44 kN and total extension of 50 mm as is shown in Figure 3(b).

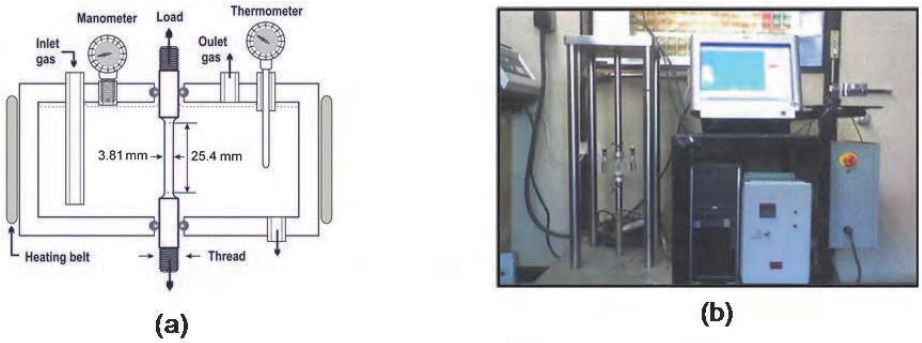

Fig. 3. (a) Autoclave and (b) M-CERT machine used to perform the SSRT.

3.3 SCC susceptibility of API X52 and X70 pipeline steels

The susceptibility to SCC in a sour solution saturated with H_2S (commonly called as sulphide stress corrosion cracking, SSCC), of API X52 and X70 steels was studied using SSRT. SCC tests were performed in samples which include the longitudinal weld bead of the pipeline steels. The SSRT tests were performed at room temperature in air and with the NACE solution saturated with H_2S at 50°C and at room temperature, using a strain rate of $1x10^{-6}$ in/sec. Cylindrical tensile specimens were machined from the tube according to the NACE TM-0198 standard as was shown in Figure 2.

The test solution according to the standard NACE TM-0177 consists of 50 g of NaCl and 5 g of glacial acetic acid dissolved in 945 g of distilled water. The solution was subsequently saturated with H_2S at a flux rate of 100 to 200 mL/min for 20 minutes.

Table 3 shows the ultimate tensile strength (UTS), elongation (EL), percentage of reduction in area (RA), reduction in area ratio (RAR) obtained from the SSRT curves. From Table 3 can be observed that specimens tested in air showed the maximum %RA, which indicate a high ductility compared with those tested in aggressive environment. The X52 specimens tested in the NACE solution saturated with H_2S at room temperature presented the maximum susceptibility to SCC. This is in agreement with results reported in the literature (Lopez *et* al, 1996; NACE TM 0177, 2005; Perdomo *et* al, 2002). Meanwhile, the maximal susceptibility to SCC in X70 specimens tested in NACE solution saturated with H_2S was at 50 °C.

SSRT tests are widely used to evaluate the susceptibility to stress corrosion cracking of various materials (Wang *et* al, 2001; Casales *et* al, 2000, 2004; Parking & Beavers, 2003; Chen

et al, 2002; Wang *et* al, 2002; Zhang *et* al, 1999; Brongers *et* al, 2000; Park *et* al, 2002; Beavers & Koch, 1992; Liou *et* al, 2002). The failure time for samples tested in air, NACE solution at 20°C and NACE solution at 50°C was around 45, 20, 27 and 41, 23 and 39 hours for the X52 and X70 steels respectively. It is clear that specimens tested in the sour solution saturated with H_2S presented high susceptibility to SCC. Corrosion was found to be an important factor in the initiation of some of the cracks. The susceptibility to SCC was manifested as a decrease in the mechanical properties, e.g., strain values before failure, ultimate tensile strength, reduction in area, time to failure and in some cases the presence of secondary cracking along the gauge length of the specimen.

Steel	Environment	UTS (MPa)	EL (mm)	%RA	RAR	Failure zone
X52	Air	391	2.03	55.6	N/A	Base Metal
	NACE+H_2S at 25ºC	249	1.42	13.8	0.248	Weld bead/HAZ
	NACE+H_2S at 50ºC	233	1.88	7.25	0.130	Weld bead/HAZ
X70	Air	462	2.64	50.98	N/A	Weld bead
	NACE+H_2S at 25ºC	213	1.21	6.91	0.135	Weld bead
	NACE+H_2S at 50ºC	355	2.03	4.38	0.085	Weld bead/HAZ

Table 3. Summary of the SSRT results to evaluate the SCC susceptibility.

The susceptibility to SCC depends on many factors such as: alloying elements (Kim *et* al, 1998) microstructure (Wilhelm & Kane, 1984), applied stresses (Miyasaka *et* al, 1996), environments (Vangelder et al, 1987), temperature (Casales *et* al, 2002), strength (López *et* al, 1996), strain (Parkins, 1990), among others.

In the SSR tests, the specimens tested in air exhibited a ductile type of failure. Whereas, in the corrosive solution, the specimens shown a brittle fracture. Among all testing environments, the NACE solution saturated with H_2S had strong influence on SSRT results, reflected in the degradation of mechanical properties. Both steels presented a corrosive attack in the form of anodic dissolution of the material. The X52 steel showed the best resistance to the corrosive attack. All the cracks, primary and secondary were perpendicular to the applied tension axis, being indicative of SSCC.

These cracks were related to the diffusion of atomic hydrogen promoting the embrittlement damage. The failure in air occurred in some cases in the weld joint, but in presence of the NACE solution saturated with H_2S the failure always occurred in the HAZ. The path of the crack was very irregular with brittle appearance.

The failure in air occurred in some cases in the base metal (BM) for the X52 steel, meanwhile, for the X70 occurs in the weld bead (WB) as is observed in Figure 4(a). In presence of the NACE solution the failure always occurred in the heat affected zone (HAZ) (Figure 4b and 4c). The major occurrence of those fractures, is related to the higher stress concentration by the lost metal regions by anodic dissolution (pits and general corrosion) and the diffusion of atomic hydrogen into the entrapping sites during the welding process and also to microstructural trappings.

Additionally, the diffusion of hydrogen and the stresses focused in the surrounding of the crack initiations sites develop the initiation and the growing of cracks (Contreras *et* al, 2005). The mode of crack growth was discontinuous, observing little deformation and the

formation of a neck in the failure zone was absent for the tests performed in the NACE solution, which it is related to the brittle fracture. The SCC of low strength steels is characterized by transgranular fracture, in contrast to intergranular fracture of high strength steels (Shim & Byrne, 1990; Asahi *et* al, 1988; Tsay *et* al, 2000).

Fig. 4. Optical macrographs of the longitudinal sections (X70 steel) of the specimens after cracked, showing the zone where they failed: (a) tested in air, (b) tested in NACE solution at 25ºC and (c) tested in NACE solution at 50ºC

Mechanical fracture techniques have been used to quantify the stress effects and the sour environment effects in the cracking. Figure 5 shows SEM micrographs of the near surface cross-section micrographs in the failed SSRT specimens tested in the NACE solution saturated with H_2S. The path of the crack was very irregular with brittle appearance (Figure 5a). In addition, it is observed that X70 steel is more susceptible to the corrosion attack as shown in Figure 5(b), showing secondary cracks after being fractured in a NACE solution saturated with H_2S at 50ºC. It was observed that at 25ºC, the attack was in the pitting form and it was less severe than at 50ºC. Meanwhile, at 50°C the attack was in the form of micro-cracks (Fig. 5b) and it was more homogeneous along the gauge section of the specimen.

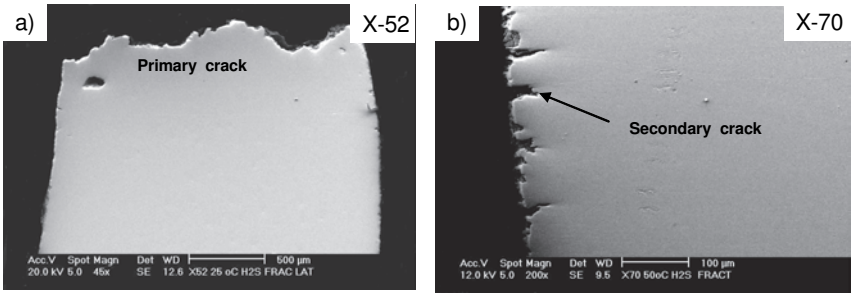

Fig. 5. SEM micrographs of tensile fractured samples (a) X52 steel showing the appearance of the fracture surface (primary crack) tested at 25°C, and (b) X70 steel showing the secondary cracks in the longitudinal gauge section, tested at 50°C.

3.4 Effect of multiple repairs in girth welds of API X52 pipeline on SCC

3.4.1 Slow strain rate tests carried out in NACE solution

Sulphide stress corrosion cracking (SSCC) susceptibility of four conditions of shielded metal arc welding repairs and one as welded specimen of the girth weld in seamless API X52 PSL2 steel pipe was evaluated using SSRT. The SSR tests were performed in air and in a sour solution saturated with H_2S both at room temperature to a constant elongation rate of $1x10^{-6}$ in/sec. The SSCC susceptibility was evaluated in function of the reduction in area ratio and elongation plastic ratio and also was manifested as a decrease in the mechanical properties. The dimensions of the line pipe were 8 inches (203.2mm) in diameter and 0.437 inches (11.1mm) in nominal wall thickness, with V-bevel at 30° in the welding. The chemical composition was showed in Table 1 (X52-B). The girth welds were obtained from the quality control department of the company Construcciones Maritimas Mexicanas (CMM-PROTEXA), carried out by qualified welders under a qualified welding procedure according to API 1104 standard (API 1104, 2005), using the SMAW process, with a 0.125 inch in diameter consumable filler rod E-6010 for the root and hot pass and with a 0.185 inches electrode E-7010G for the subsequent passes. The original weld (0R) was repaired by arc air and hand disc grinder to a depth between the root and hot pass and rewelding using the same welding procedure (1R). To simulate multiple welding repairs, the repaired weld was similarly removed and welded again, to obtain a second (2R), third (3R) and fourth (4R) welding repair. X-ray inspection was used to verify the quality of the welded unions after each welding repair according to the requirements of API-1104.

Several tests (SSRT) were carried out for each one of the welding repair conditions, for both, in air and NACE solution. Profiles obtained from the SSRT are shown in Figure 6.

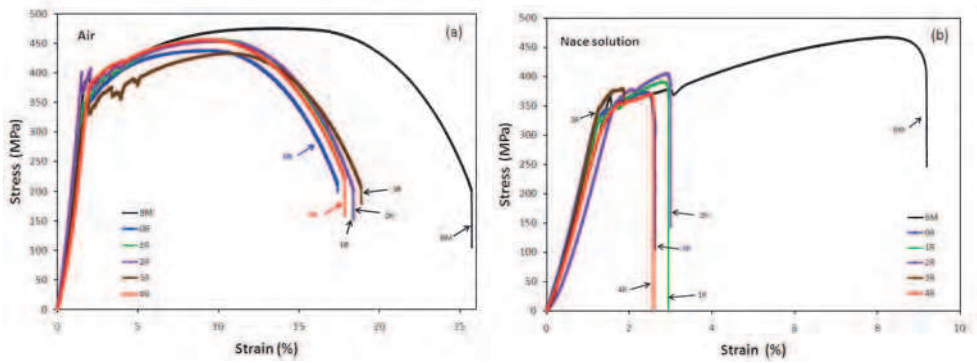

Fig. 6. Stress versus strain profiles obtained from SSRT for all repair conditions (a) Tested in air; (b) tested in NACE solution saturate with H_2S at room temperature.

SCC susceptibility was evaluated of the results obtained from SSRT according to NACE TM 0198 and ASTM G129. The results are showed in Table 4. The strength, elongation and reduction in area decreases significantly when the samples are exposed to the NACE solution saturate with H_2S. This behavior could be attributed to combined action between tensile stress and the specific corrosive environment. In fact, the synergic effect between the stress, chloride and sulphide (obtained of hydrogen sulphide) increased significantly the susceptibility to SSCC.

According to the results of RAR and EPR is clear that the specimens tested in the NACE solution saturated with H_2S exhibited high susceptibility to SSCC. It is suggested that decrease in mechanical properties is due to a hydrogen embrittlement mechanism, because the fractured samples showed little deformation in the gauged section and there is not formation of neck in the failure zone. From the different welding repair conditions, the second repair showed the best performance and behavior in the tests, for both, in air and in the NACE solution.

Condition	Environment	RA, %	EP, %	RAR	EPR	Failure zone
Base metal	Air	87.62	23.26			
As welded	Air	83.16	15.00			BM
First repair	Air	86.86	16.18			BM
Second repair	Air	86.88	16.69			BM
Third repair	Air	82.30	14.37			BM
Fourth repair	Air	86.34	15.51			BM
Base metal	NACE Solution	10.40	4.92	0.118	0.211	
As welded	NACE Solution	6.17	1.34	0.074	0.089	ICHAZ
First repair	NACE Solution	7.84	1.22	0.090	0.075	ICHAZ
Second repair	NACE Solution	9.30	1.65	0.107	0.098	ICHAZ
Third repair	NACE Solution	4.87	0.689	0.059	0.047	ICHAZ
Fourth repair	NACE Solution	5.26	0.984	0.060	0.063	ICHAZ

Table 4. Summary of the SSRT results to evaluate the SCC susceptibility of multiple repairs in girth welds of API X52

According to Lant *et* al. (Lant *et* al, 2001) the temper bead technique generates overlap beads producing grain refinement in the coarse grained heat affected zone (CGHAZ) of the previous bead and decreases the residual stresses due to the input of additional thermal energy. Considering this assumption, this it is the reason for which the second welding repair presents the best mechanical behavior, for both, in air and in NACE solution.
The microstructure as well as the mechanical properties obtained for the different weld repair conditions were shown elsewhere (Vega *et* al, 2008). Micrographs of the fracture surface specimens were shown elsewhere (Vega *et* al, 2009). In air, all the specimens exhibited a ductile type of failure (the presence of quasi-cleavage fracture mixed with microvoid coalescence was observed). Meanwhile, in NACE solution saturated with H_2S showed a brittle fracture with a transgranular appearance. The brittle fracture is related to the higher stress concentration by the lost metal regions due to anodic dissolution (pits and general corrosion) and the diffusion of atomic hydrogen into the entrapping sites during the welding process. Additionally, the diffusion of hydrogen and the stresses close to the crack initiations sites develop the initiation and the growing of cracks.
The specimens tested in air for the different conditions of repair, the failure occurred in the BM very close to the interface with the HAZ. For the samples tested in the NACE solution for all the repair conditions, the failure occurred mainly along the intercritical heat affected zone (ICHAZ) as is shown in Figure 7.

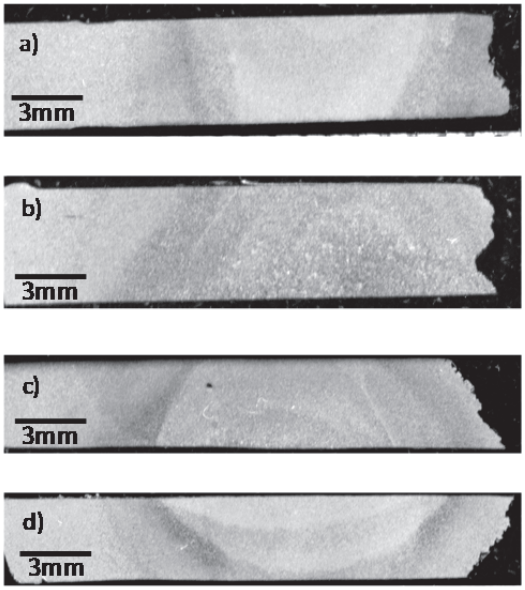

Fig. 7. Optical micrographs of longitudinal section of fracture samples from SSRT showing failure zone of specimens tested in NACE solution at room temperature, a) first repair; b) second repair; c) third repair; d) fourth repair

SSCC in steels and in welded line pipes of low and medium strength has also been denominated as stress oriented hydrogen induced cracking (SOHIC) (Takahashi, 1995, 1996a, 1996b; Carneiro, 2003). The SOHIC is divided in two stages: in the first stage, cracks parallel to applied stress are formed by the hydrogen induced cracking (HIC) mechanism; in the latter stage, the cracks link perpendicularly to applied stress like SSCC. All the found cracks in the different welding repair conditions agree with the theory proposed by the SOHIC mechanism; cracks formed parallel to the applied stress after link with cracks formed perpendicular to the direction of the applied stress, preferentially induced along the ICHAZ as is shown in Figure 8.

Most of the failures reported by SSCC or SOHIC in welded line pipes of low and medium strength have occurred in the ICHAZ (Kimura, 1989; Takahashi, 1996; Endo, 1994). According to Takahashi *et* al. (Takahashi, 1996) the applied stress acts to enhance shear stress around the first parallel formed cracks to the stress and the shear stress can cause local yielding which facilitates the vertical linking of the parallel cracks to break the specimen eventually.

McGaughy *et* al. (McGaughy, 1992; McGaughy & Boyles, 1990) evaluated the effects of SMAW repairs on the residual stress distribution of girth welds in API 5L X65 line pipe. The girth welds contained repairs which included a single, double and a full wall repair. The results showed that increasing number of welding repairs increased the level of axial and hoop residual stresses, inside and outside surface of the line pipe. This suggested that the contribution of the residual stresses together with the presence of discontinuities near to the fracture interface makes the WB/HAZ interface more susceptible zone to SCC.

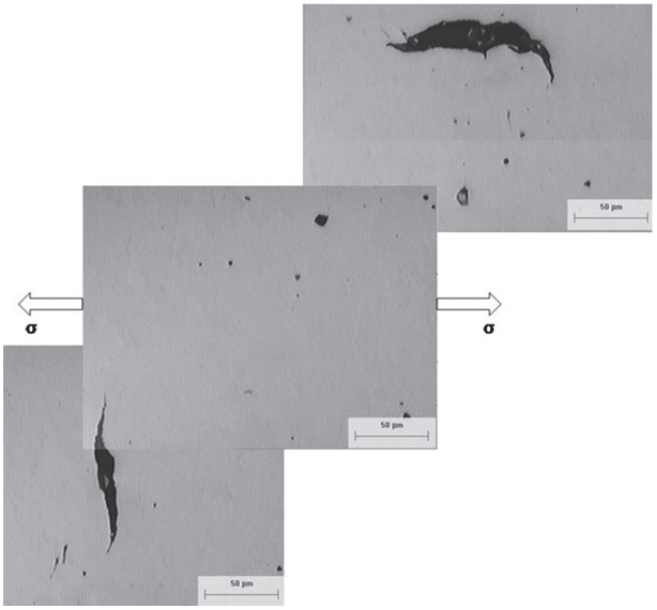

Fig. 8. Scanning electron microscopy images showing parallel and perpendicular cracks found along ICHAZ (sample with third repair).

3.4.2 Slow strain rate tests carried out in NS4 solution

The susceptibility to SCC in girth welds of seamless API X52 steel pipe containing multiple shielded metal arc welding (SMAW) repairs and one as-welded condition were evaluated using SSRT according to NACE TM-0198 standard. The SSRT were performed in air and NS4 solution at pH 10 (basic) and pH 3 (acid) at room temperature and at constant elongation rate of $1x10^{-6}$ in/sec. Cylindrical tensile specimens were transversal machined to the direction of the application to the girth weld. The specimens according to the number of repairs were identified as 0R (as-welded), 1R, 2R, 3R and 4R respectively.

The experimental research about SCC in pipelines considering the external environment have been studied using NS4 solutions (Elboujdaini *et* al, 2000; Pan *et* al, 2006; Bulger & Luo, 2000; Fang *et* al, 2007; Lu & Luo, 2006), this as results of investigations about the chemical composition of the solution on the surface of the pipeline failed by SCC. The main goal using NS4 solution is to simulate the chemical composition of the soil. The great majority of these studies were made in the base metal of pipeline steels; there are few studies on the longitudinal and circumferential welding but none reported in function of the number of repairs. The chemical composition of the soil solution use to carry out the SSRT is shown in Table 5.

Stress vs. Strain profiles obtained from the SSRT performed performed in air and in the NS4 solution both at room temperature for the different welding repair conditions are shown in Figure 9. Base metal (BM) presented the maximum strain for SSRT carried out in air (26%) and in NS4 solution (20% with pH 3 and 23% with pH 10) in comparison with the four weldments. Specimens tested in air showed a strain about 16-19% meanwhile the specimens tested in NS4 showed a strain between 14-19% with pH 3 and pH 10 respectively.

Compound	Composition (gr/L)
Sodium bicarbonate ($NaHCO_3$)	0.483
Calcium chloride ($CaCl_2$)	0.137
Magnesium sulfate ($MgSO_4$)	0.131
Potassium chloride (KCl)	0.122

Table 5. Chemical composition of the NS4 solution

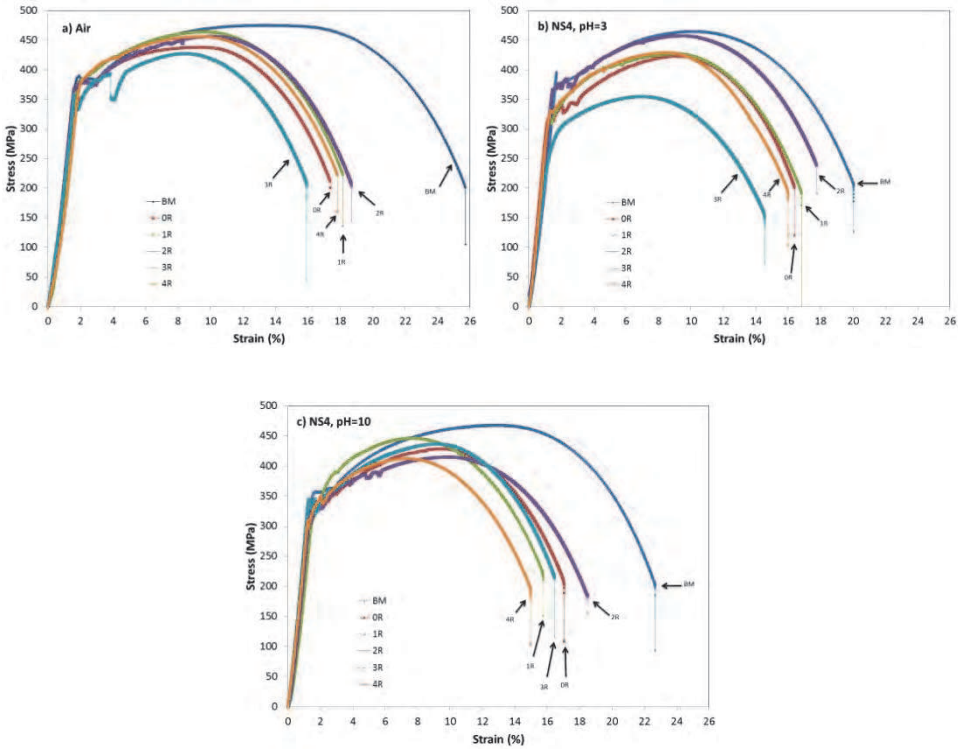

Fig. 9. Stress versus strain profiles obtained from the SSRT in function of pH and number of repairs, a) in air, b) in NS4 solution with pH 3 and c) in NS4 solution with pH 10.

From the analysis of these curves we obtain results of reduction in area (RA), plastic elongation (EP), reduction in area ratio (RAR) and elongation plastic ratio (EPR) which are shown in Table 6. RAR and EPR were calculated according to NACE TM 0198. Ratios in the range of 0.8-1.0 indicate that steel has high resistance to SCC, whereas low values (i.e. <0.5) show high susceptibility.

Condition	Environment	YS (MPa)	UTS (MPa)	RA (%)	E_p (%)	RAR	EPR
BM	Air	386.1	475.2	89.10	23.26		
0 rep		356.0	437.5	85.74	15.00		
1º rep		379.9	464.2	88.10	16.18		
2º rep		384.1	456.2	88.53	16.69		
3º rep		359.7	427.4	84.60	14.37		
4º rep		379.2	455.9	86.34	15.51		
BM	NS4, pH=3	396.8	464.8	88.13	19.72	0.98	0.84
0 rep		325.9	423.0	84.10	14.17	0.98	0.94
1º rep		322.5	427.5	86.84	15.47	0.98	0.95
2º rep		351.8	438.2	86.90	16.69	0.98	1.00
3º rep		318.1	354.9	83.91	13.78	0.99	0.95
4º rep		329.7	428.8	85.01	15.00	0.98	0.96
BM	NS4, pH=10	357.0	467.7	87.62	18.34	0.98	0.78
0 rep		316.0	428.4	83.16	14.98	0.96	0.99
1º rep		324.9	446.3	86.86	15.51	0.98	0.95
2º rep		340.6	415.2	86.88	16.22	0.98	0.97
3º rep		344.6	436.8	82.30	12.99	0.97	0.90
4º rep		318.0	412.1	86.10	14.60	0.99	0.94

Table 6. Assessment of the susceptibility to SCC obtained from the SSR tests

According to these results, it is clear that the specimens tested in the NS4 solution not exhibited susceptibility to SCC. In addition, secondary cracks or corrosion were not observed in the specimens after made the SSR tests. The strength, elongation and reduction in area decreases slightly when the samples are exposed to the NS4 solution.

Passive film rupture, anodic dissolution and repassivation are the generally accepted mechanism on SCC, but this is dependent on the strain rate. If the strain rate is too high, the material fails predominantly under mechanical loading, and the environment did not have time to damage the material. By other hand, at too slow strain rate the passive film formed over a longer period of time will be too dense to be ruptured by the slow strain rate.

SEM observations of the fracture surfaces of specimens tested in air and NS4 solution with pH of 3 and 10 showed microvoids coalescence for all the conditions studied which is characteristic of a ductile type of fracture. Figure 10 shows SEM images of the fracture surface after SSRT were performed.

As the strain increases the neck formation in the gauge section before the samples failed was observed. This was reflected in the assessment of reduction area on the fracture surface. On the edge of the fracture surface an intergranular type of fracture was observed, towards the centre of the fracture change to a ductile type.

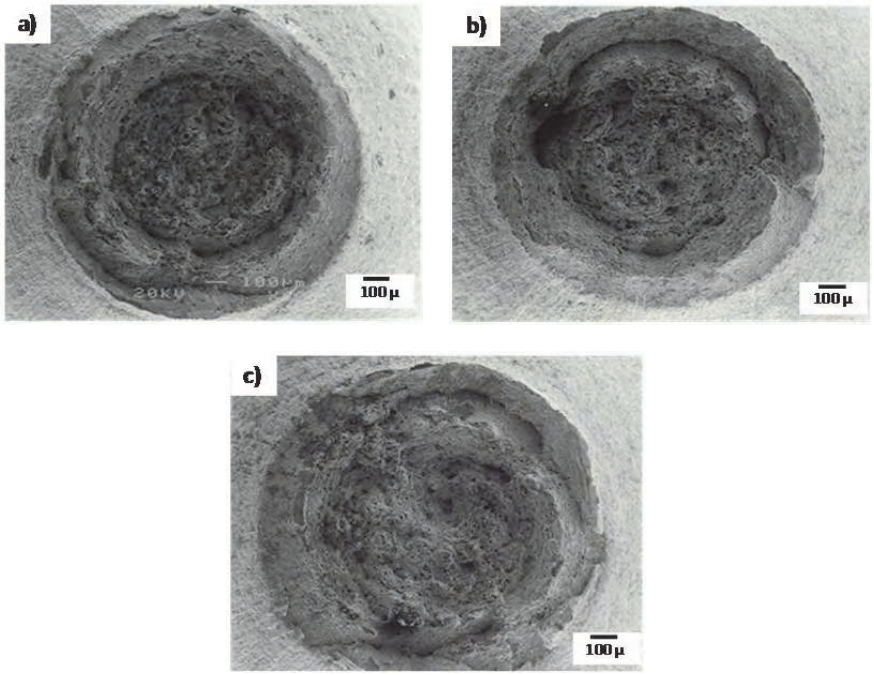

Fig. 10. Fracture surfaces after made the SSRT, a) in air, b) NS4 solution with pH 3 and c) NS4 solution with pH-10.

Optical micrographs of the longitudinal sections for specimens tested in NS4 solution with pH-10 showing the failure zone are shown in Figure 11. The specimens tested in NS4 solution with pH of 3 and 10 for the different conditions of repair, the failure occurred in the BM/HAZ interface without presence of secondary cracks in the gauge section.

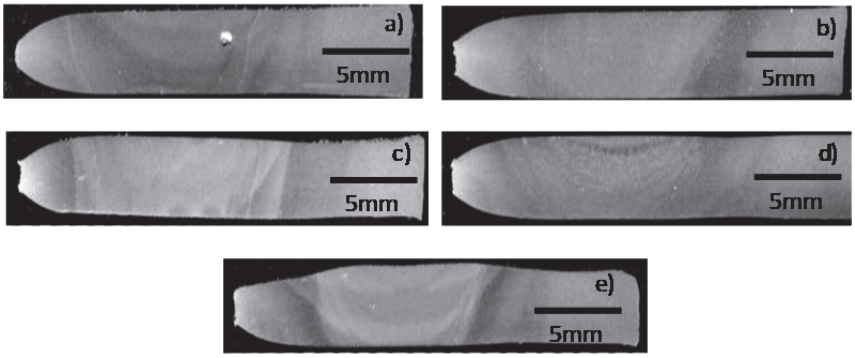

Fig. 11. Optical micrographs of longitudinal section of fractured samples from SSRT performed in NS4 solution with pH-10 showing failure zone, a) as welded; b) first repair; c) second repair; d) third repair; e) fourth repair.

The results showed that increasing number of welding repairs increased the level of axial and hoop residual stresses, inside and outside surface of the line pipe. The SCC susceptibility was expressed in function of the reduction in area ratio and elongation ratio. The yield strength, tensile strength and ductility of the welded joints shown a decrease when they are exposed to the NS4 solution. The metallographic observations of the fractured specimens show that the most susceptibility area to SCC was the BM/HAZ interface.

3.5 SCC susceptibility of API X60 and X65 pipeline steels

The SCC susceptibility of API X60 and X65 longitudinal weld beads was evaluated using SSRT in a brine solution saturated with H_2S at room temperature (25°C), 37°C and 50°C. The tests were supplemented by potentiodynamic polarization curves and hydrogen permeation measurements. Longitudinal weld beads produced by SMAW process were analyzed. The chemical composition of these steels was shown in Table 1. These types of pipes are typically used in the Mexican pipeline systems for transporting hydrocarbons.
Figure 12 shows micrographs of the X60 and X65 steels weldments. These figures clearly show the different microstructures found in a weldment, which consists mainly of polygonal and coarse acicular ferrite. This microstructure optimizes the strength and the toughness of the weld beads (Bhatti, 1984; Dolby, 1976; Kirkwood, 1978; Asahi, 1994).

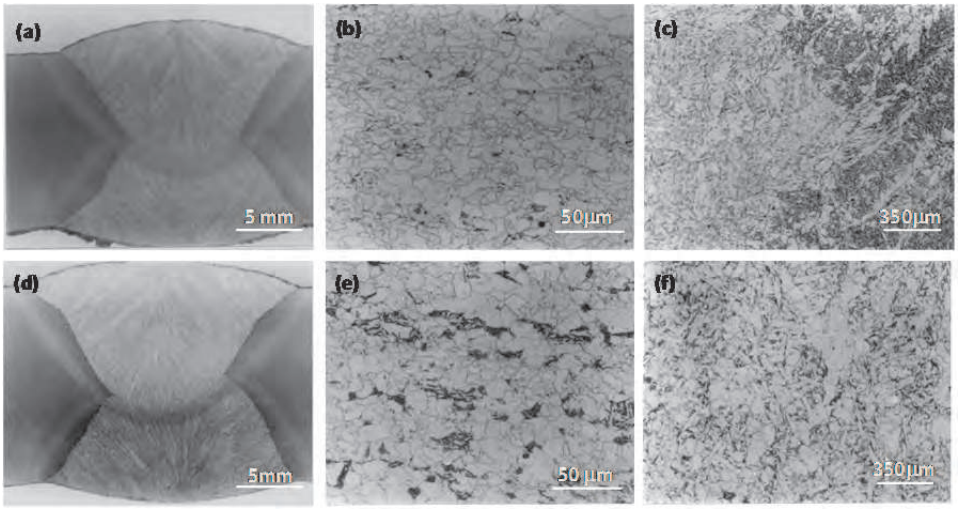

Fig. 12 Microstructures obtained by optical microscopy of the weld bead: (a-c) API X60 steel, (d-f) API X65 steel.

The welding industry has recognized that weld induced stresses play an important role in SCC phenomena. Each year, tens of millions of dollars are expended to replace or repair pipes and vessels that suffer SCC or hydrogen embrittlement (HE). When H_2S is present in the pipelines transporting hydrocarbons, this type of brittle failure is known as sulfide stress corrosion cracking, and it has been established as a particular case of hydrogen embrittlement (Tsay et al, 2000). The transport of these types of products always induces failures in the pipeline systems, and is very frequently in the weld beads.

The development of multi-phase microstructures is important for the attainment of certain mechanical properties, but it can be detrimental for resistance to SSCC. Carbon-rich phases such as pearlite, bainite, or martensite can be particularly susceptible to this mode of HE. The susceptibility toward SSCC was measured with the I_{SSCC} index according to:

$$I_{SSCC} = \frac{\%RA_{AIR} - \%RA_{NACE}}{\%RA_{AIR}} \quad (6)$$

where $\%RA_{AIR}$ and $\%RA_{NACE}$ are the percentage reduction in area values in air and in the NACE solution saturated with H_2S. The results are plotted in Figure 13(a). Values close to the unit mean that the steel is highly susceptible to SCC, whereas values close to zero mean that the steel is immune to SSCC. Thus, Figure 13(a) clearly shows that, in all cases, regardless of the temperature, both steels are highly susceptible to SCC, and the effect of the temperature is negligible, although the tendency is that this susceptibility increases with increasing temperature. X60 pipeline steel was more susceptible to SCC than the X65 steel, although this difference seems to be negligible.

Hydrogen permeation tests were carried out using the two-component Devanathan-Stachurski cell (Devanathan & Stachurski, 1962). Figure 13(b) shows the effect of the temperature on the hydrogen uptake (C_0) for both steels. It is clear that the amount of hydrogen uptake increases with temperature for both steels, being always higher in the X60 than in the X65 steel. All these results are consistent with those found in the literature (Asahi *et* al., 1994). The corrosion rate, taken as the corrosion current density, I_{corr}, the amount of hydrogen uptake for the weldments, C_0, and the SSCC susceptibility increased with an increase in the temperature from 25°C to 50°C. Although anodic dissolution seems to play an important role in the cracking mechanism, the most likely mechanism for the cracking susceptibility of X60 and X65 weldments in H_2S solutions seems to be hydrogen embrittlement (Natividad *et* al., 2006).

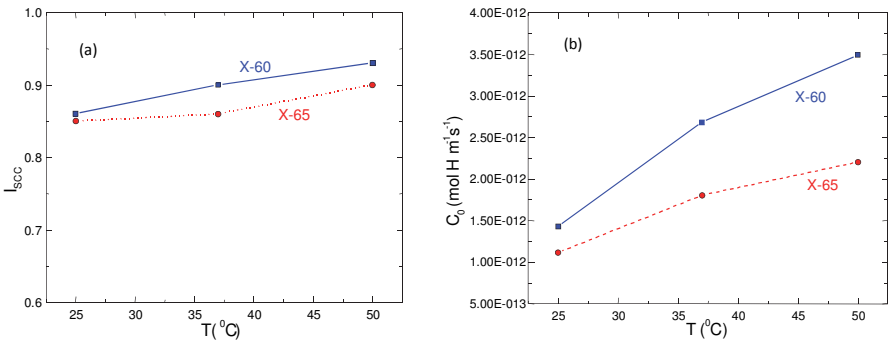

Fig. 13. (a) Effect of temperature on the I_{SSCC} values for both steels and (b) on the hydrogen uptake for both steels.

Potentiodynamic polarization curves were performed at a sweep rate of 1.0 mV/s using a fully automated potentiostat controlled with a desktop computer. The scanning started at –500 mV, with respect to E_{corr}, and finished at 300 mV more positive than E_{corr}, at a scanning rate of 1 mV/s. Corrosion current values (I_{corr}) were calculated using Tafel extrapolation.

Figure 14 show the effect of temperature on the polarization curves for X60 and X65 pipeline steels. As expected in these solutions, there is no passive region in any of the cases, only

active dissolution. For both steels, the E_{corr} decreases as the temperature is increased, with the most noble value at 25°C and –600 mV, and the most active at 50°C and around –800 mV. The E_{corr} value for the X60 steel at 37°C was –650 mV whereas for the X65 steel, it was –700 mV.

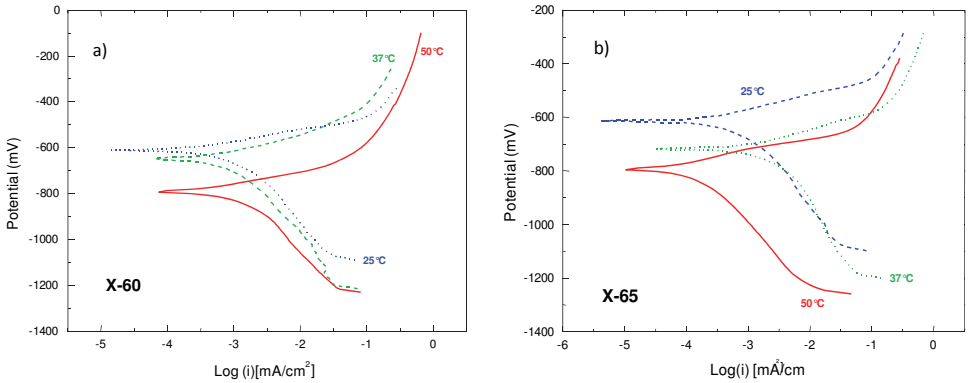

Fig. 14. Polarization curves obtained from weld bead at different temperatures in the NACE solution saturated with H_2S, (a) X60; (b) X65 steel.

Metallographic cross sections of X60 and X65 steels are shown in Figure 15. The cracks were transgranular in nature predominantly, and, just as indicated by the polarization curve that the corrosion rate increased as the temperature increased, the amount of corrosion products inside the cracks is more pronounced at 50 than at 25°C. Cross sections of the gage section of X60 steel showed secondary cracks as is shown in Figure 15(a). For X65 steel, no cracks were observed, only pits, as is shown in Figure 15(b).

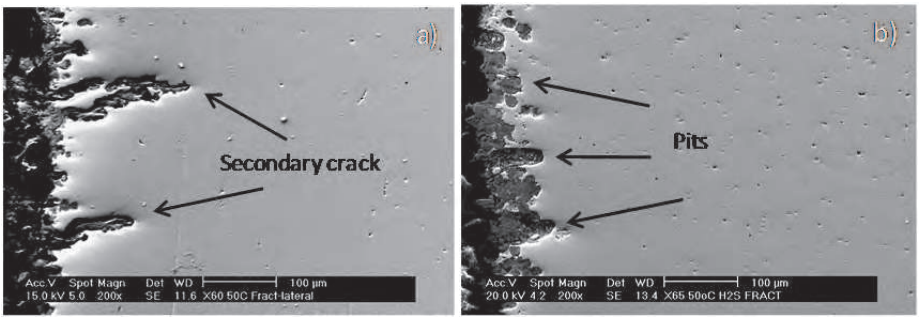

Fig. 15. Cross-sections of weldments tested in the NACE solution saturated with H_2S. (a)X60 steel at 50°C, (b)X65 steel at 50°C.

4. Conclusions

This chapter presents the mechanical and environmental effects as well as fracture characteristics on SCC susceptibility of steels used in the oil industry using SSRT. The tests were performed in samples which include the longitudinal and circumferential weld bead of pipeline steels. The steels studied are low carbon steels API X52, X60, X65 and X70. These

steels were evaluated in a brine solution saturated with H_2S according to NACE TM 0177 (to evaluate sulphide stress corrosion cracking susceptibility). Additionally, some circumferential weldments of API X52 were evaluated in NS4 solution.

The results of the SSRT carried out in API X52 and X70 steels to evaluate the SCC susceptibility revealed that specimens tested in the NACE solution saturated with H_2S at room temperature and 50°C, presented high susceptibility to SCC, reflected in the degradation of mechanical properties. The specimens tested in air exhibited a ductile type of fracture. Whereas, in the corrosive solution, the specimens shown a brittle fracture. Both steels presented a corrosive attack in the form of anodic dissolution of the material. The X52 steel showed best resistance to SCC. All the cracks, primary and secondary were perpendicular to the applied tension axis, being indicative of SCC. These cracks were related to the diffusion of atomic hydrogen promoting the embrittlement damage. The failure of samples tested in air occurred in some cases in the weld joint, but in presence of the NACE solution the failure always occurred in the HAZ.

SCC susceptibility of API X52 with multiple welding repairs in girth welds of pipelines was evaluated by means of SSRT in NACE solution saturated with H_2S. According to the results of RAR and EPR, it is clear that welding joints are susceptible to SCC. The specimens tested in air for the different conditions of repair, the failure occurred in the BM very close to the interface with the HAZ. In presence of NACE solution saturated with H_2S at room temperature, the most susceptible zone to SCC was the ICHAZ following the SOHIC. Although in presence of imperfections like pores and non-metallic inclusions near to the interface with the HAZ, fusion line becomes the most susceptible zone to SCC. Using temper bead technique contributes to the reinforcement of the mechanical behavior, improving resistance to SCC as was observed in the second welding repair. The temper bead technique generates overlap beads producing grain refinement in the coarse grained heat affected zone of the previous bead and decreases the residual stresses due to the input of additional thermal energy.

The susceptibility to SCC in girth welds of seamless API X52 steel pipe containing multiple welding repairs was evaluated using SSRT in soil solution. The SSRT were performed in air and NS4 solution at pH 10 (basic) and pH 3 (acid) at room temperature. The main goal using NS4 solution is to simulate the chemical composition of the soil. According to the RAR and EPR results, it is clear that the specimens tested in the NS4 solution not exhibited susceptibility to SCC. In addition, secondary cracks or corrosion were not observed in the specimens after perform the SSRT. The strength, elongation and reduction in area decreases slightly when the samples are exposed to the NS4 solution. SEM observations of the fracture surfaces of specimens tested in air and NS4 solution with pH of 3 and 10 showed microvoids coalescence for all the conditions studied which is characteristic of a ductile type of fracture. The metallographic observations of the fractured specimens show that the most susceptible area to SCC was the BM/HAZ interface.

The SCC susceptibility considering the effects of the temperature on the corrosion rate, and hydrogen uptake of API X60 and X65 weldments through SSRT was carried out. The SCC susceptibility and corrosion rate, taken as I_{corr}, for both weldments, increased with an increase in the temperature from 25 to 50°C, as well as the amount of hydrogen uptake for the weldments. The most likely mechanism for the cracking susceptibility of X60 and X65 weldments in sour solutions seems to be hydrogen embrittlement, but anodic dissolution seems to play an important role in the cracking mechanism. Specimens tested in NACE solution showed brittle type of fracture, with a very small percentage reduction in area values, and the gage section shown a large number of secondary cracks.

5. References

API STD 1104-2005 (R 2010) Welding of Pipelines and Related Facilities - Twentieth Edition; July 2007, 2: December 2008

Asahi, H.; Sogo, Y.; Ueno, M. & Higashiyama, H. (1988). Effects of Mn, P, and Mo on sulfide stress cracking resistance of high-strength low-alloy steels, *Metallurgical Transactions A-Physical metallurgy and materials science*, Volume 19, Issue 9 (Sep 1988), pp. 2171-2177, ISSN 0360-2133

Asahi, H.; Ueno, M. & Yonezawa, T. (1994). Prediction of Sulfide Stress Cracking in High-Strength Tubular. *Corrosion,* Volume 50, Issue 7, (July, 1994), pp. 537-545. ISSN 0010-9312

ASTM G129-2000 (R 2006) Standard practice for slow strain rate testing to evaluate the susceptibility of metallic materials to environmentally assisted cracking

Beavers, J. & Koch, G. (1992). Limitations of the slow strain rate test for stress-corrosion cracking testing, *Corrosion*, Volume 48, Issue 3 (Mar 1992), pp. 256-264, ISSN 0010-9312

Beavers, J.; & Harle, B. (2001). Mechanisms of high-pH and near-neutral-pH SCC of underground pipelines, *Journal of Offshore Mechanics and Arctic Engineering-Transactions of the ASME*, Volume 123, Issue 3 (Aug 2001), pp. 147-151, ISSN: 0892-7219

Bhatti, A.; Saggese M.; Hawkins D.; Whiteman, M. & Golding M. (1984). Analysis of Inclusions in Submerged-Arc Welds in Microalloyed Steels. *Welding Journal,* Volume 63, Issue 7, (1984), pp. S224-S230), ISSN 0043-2296

Brongers, M.; Beavers, J.; Jaske, C. & Delanty, B. (2000). Effect of hydrostatic testing on ductile tearing of X65 line pipe steel with stress corrosion cracks, *Corrosion*, Volume 56, Issue 10 (Oct 2000), pp. 1050-1058, ISSN 0010-9312

Bulger, J. & Luo, L. (2000). Effect of microstructure on near-neutral pH SCC. *Proceedings in the International Pipeline Conference ASME 2000*, Calgary, Canada, October 1-5, 2000, ISBN 10 0791816664

Carneiro, R.; Ratnapuli, R. & Lins, V. (2003). The influence of chemical composition and microstructure of API line pipe steels on hydrogen induced cracking and sulfide stress corrosion cracking, *Materials science and engineering A-Structural materials properties microstructure and processing*, Volume 357, Issue 1-2 (Sep 2003), pp. 104-110, ISSN 0921-5093

Casales, M.; Espinosa-Medina, M.; Martinez-Villafañe, A.; Salinas-Bravo, V. & Gonzalez-Rodríguez, J. (2000). Predicting susceptibility to intergranular stress corrosion cracking of Alloy 690, *Corrosion*, Volume 56, Issue 11 (Nov 2000), pp. 1133-1139, ISSN 0010-9312

Casales, M.; Salinas-Bravo, V.; Espinosa-Medina, M.; Martinez-Villafañe, A. & Gonzalez-Rodríguez, J. (2004). Electrochemical noise generated during the stress corrosion cracking of sensitized alloy 690, *Journal of Solid State Electrochemistry*, Volume 8, Issue 5 (Apr 2004), pp. 290-295, ISSN 1432-8488

Casales, M.; Salinas-Bravo, V.; Martinez-Villafañe, A. & Gonzalez-Rodríguez, J. (2002). Effect of heat treatment on the stress corrosion cracking of alloy 690, *Materials Science and Engineering A-Structural materials properties microstructure and processing*, Volume 332, Issue 1-2 (Jul 2002), pp. 223-230, ISSN 0921-5093

Chen, W.; King, F. & Vokes, E. (2002). Characteristics of near-neutral-pH stress corrosion cracks in an X65 pipeline, *Corrosion*, Volume 58, Issue 3 (Mar 2002), pp. 267-275, ISSN 0010-9312

Contreras, A.; Albiter A., Salazar M., Pérez R. (2005). Slow strain rate corrosion and fracture characteristics of X52 and X70 pipeline steels, *Materials Science Engineering A,* Volume 407 (2005) pp. 45-52, ISSN 0921-5093

Craig, B. (1998). Calculating the lowest failure pressure for electric resistance welded pipe, *Welding Journal,* Volume 77, Issue 1 (Jan 1998), pp. 61-63, ISSN: 0043-2296

Delanty, B. & O'Beirne, J. (1992). Major field-study compares pipeline SCC with coatings, *Oil & Gas Journal,* Volume 90, Issue 24, (Jun 1992), pp. 39-44, ISSN: 0030-1388

Devanathan, M.A.V., Stachurski Z., Proc. R. Soc. London A 270 (1962): p. 90.

Dolby, R. (1976). Factors Controlling Weld Toughness-The Present, Position, Pt. II-Weld Metals. The Welding Institute Members Report 14/1976/M (May, 1976). London

Elboujdaini, M.; Wang, Y. & Revie, R. (2000). Initiation of stress corrosion cracking on X65 line pipe steels in near-neutral pH environment, *Proceedings of the International Pipeline Conference ASME 2000,* Calgary, Canada, October 1-5, 2000, ISBN 10 0791816664

Endo, S.; Nagae, M.; Kobayashi, Y. & Ume, K. (1994). Sulfide stress-corrosion cracking in welded-joints of welded line pipes, *ISIJ International,* Volume 34, Issue 2 (1994), pp. 217-223, ISSN 0915-1559

Fang, B.; Atrens, A.; Wang, J.; Han, E.; Zhu, Z. & Ke, W. (2003). Review of stress corrosion cracking of pipeline steels in "low" and "high" pH solutions, *Journal of Materials Science*, Volume 38, Issue 1 (Jan 2003), pp. 127-132, ISSN: 0022-2461

Fang, B.; Eadie, R.; Chen, W. & Elboujdaini, M. (2010). Pit to crack transition in X52 pipeline steel in near neutral pH environment Part 1-formation of blunt cracks from pits under cyclic loading, *Corrosion Engineering, Science and Technology,* Volume 45, Issue 4 (Aug 2010), pp. 302-312, ISSN: 1478-422X

Fang, B.; Han, E.; Wang, J. & Ke, W. (2007). Mechanical and environmental influences on stress corrosion cracking of an X70 pipeline steel in dilute near-neutral pH solutions, *Corrosion*, Volume 63, Issue 5 (May 2007), pp. 419-432, ISSN 0010-9312

Greer, J. (1975). Factors affecting sulfide stress cracking performance of high-strength steels, *Materials Performance*, Volume 14, Issue 3 (1975), pp. 11-22, ISSN 0094-1492

Jones, R. (1992). *Stress Corrosion Cracking,* Edited by Russell H. Jones, ASM International, 1-40, ISBN 0-87170-441-2, Ohio, U.S.A.

Kane, R.D.; Joia C.J.B.M.; Small A.L.L.T. & Ponciano J.A.C (1997). Rapid Screening of Stainless Steels for Environmental Cracking, *Materials Performance*, Volume 36, Issue 9 (Sep. 1997), pp. 71-74, ISSN 0094-1492

Kim, K.; Zhang, P.; Ha, T. & Lee, Y. (1998). Electrochemical and stress corrosion properties of duplex stainless steels modified with tungsten addition, *Corrosion*, Volume 54, Issue 11 (Nov 1998), pp. 910-921, ISSN: 0010-9312

Kimura, M.; Totsuka, N.; Kurisu, T.; Amano, K.; Matsuyama, J. & Nakai, Y. (1989). Sulfide stress-corrosion cracking of line pipe, *Corrosion,* Volume 45, Issue 4 (Apr 1989), pp. 340-346, ISSN 0010-9312

Kirkwood, P. (1978). Microstructural and Toughness Control in Low-Carbon Weld Metals. *Metal Construction,* Volume 10, Issue 5, (1978), pp. 260-264, ISSN 0307-7896

Krist, K & Leewis, L. (1998). GRI research - Stress corrosion cracking mechanisms in pipelines. *Pipeline & Gas Journal,* Volume 225, Issue 3, (Mar, 1998), pp. 49-52, ISSN 0032-0188

Lant, T.; Robinson, D.; Spafford, B. & Storesund (2001). Review of weld repair procedures for low alloy steels designed to minimize the risk of future cracking, *International journal of pressure vessels and piping,* Volume 78, Issue 11-12 (Nov-Dec 2001), pp. 813-818, ISSN 0308-0161

Leis, B.N. & Eiber R.J. (1997). Stress-Corrosion Cracking on Gas-Transmission Pipelines: History, Causes and Mitigation, Proceedings of First International Business Conference on Onshore Pipelines, (Berlin, December 1997).

Liou, H.; Hsieh, R. & Tsai, W. (2002). Microstructure and stress corrosion cracking in simulated heat-affected zones of duplex stainless steels, *Corrosion Science*, Volume 44, Issue 12 (Dec 2002), pp. 2841-2856, ISSN 0010-938X

Liu, Z.Y., Li X.G., Du C.W., Zhai G.L. & Cheng Y.F. (2008). Stress corrosion cracking behavior of X70 pipe steels in an acid soil environment, *Corrosion Science,* Volume 50, (2008), pp. 2251-2257, ISSN 0010-938X

López, H.; Raghunath, R.; Albarran, J. & Martinez, L. (1996). Microstructural aspects of sulfide stress cracking in an API X-80 pipeline steel, *Metallurgical and materials transactions A-Physical metallurgy and materials science*, Volume 27, Issue 11 (Nov 1996), pp. 3601-3611, ISSN 1073-5623

Lu, B. & Luo, J. (2006). Relationship between yield strength and near-neutral pH stress corrosion cracking resistance of pipeline steels - An effect of microstructure *Corrosion*, Volume 62, Issue 2 (Feb 2006), pp. 129-140, ISSN 0010-9312

Manfredi C. & Otegui J.L. (2002). Failures by SCC in buried pipelines, *Engineering Failure Analysis,* Volume 9, (2002), pp. 495-509, ISSN 1350-6307

McGaughy T. and L. Boyles. Significance of changes in residual stresses and mechanical properties due to SMAW repair of girth welds in line pipe, Technical Report PR-185-905, Edison Welding Institute, Columbus, OH, USA, 1990, 1–18.

McGaughy T. The influence of weld repairs on changes in residual stress and fracture toughness in pipeline girth welds. Recent Advances in Structural Mechanics, ASME 1992; PVP, Volume 248, pp. 81–86.

Miyasaka, A.; Kanamaru, T. & Ogawa, H. (1996). Critical stress for stress corrosion cracking of duplex stainless steel in sour environments, *Corrosion,* Volume 52, Issue 8 (Aug 1996), pp. 592-599, ISSN 0010-9312

NACE TM 0177-2005 Laboratory testing of metals for resistance to sulfide stress cracking and stress corrosion cracking in H_2S environments - Item No: 21212

NACE TM 0198-2004 Slow strain rate test method for screening corrosion-resistant alloys (CRAs) for stress corrosion cracking in sour oilfield service - Item No: 21232

Natividad, C.; Salazar, M.; Contreras, A.; Albiter, A.; Pérez, R. & Gonzalez-Rodríguez, J.G. (2006). Sulfide Stress Cracking Susceptibility of Welded X60 and X65 Pipeline Steels. *Corrosion,* Vol. 62, Issue 5, (May 2006), pp. 375-382, ISSN 0010-9312

Nishimura, R. & Maeda, Y. (2004). SCC evaluation of type 304 and 316 austenitic stainless steels in acidic chloride solutions using the slow strain rate technique, *Corrosion Science,* Volume 46, Issue 3 (Mar 2004), pp. 769-785, ISSN 0010-938X

Pan, B.; Peng, X.; Chu, W.; Su, Y. & Qiao, L. (2006). Stress corrosion cracking of API X60 pipeline in a soil containing water, *Materials science and engineering A*, Volume 434, Issue 1-2 (Oct 2006), pp. 76-81, ISSN 0921-5093

Park, J.; Pyun, S.; Na, K.; Lee, S. & Kho, Y. (2002). Effect of passivity of the oxide film on low-pH stress corrosion cracking of API 5L X65 pipeline steel in bicarbonate solution, *Corrosion*, Volume 58, Issue 4 (Apr 2002), pp. 329-336, ISSN 0010-9312

Parkins, R. & Beavers, J. (2003). Some effects of strain rate on the transgranular stress corrosion cracking of ferritic steels in dilute near-neutral-pH solutions, *Corrosion*, Volume 59, Issue 3 (Mar 2003), pp. 258-273, ISSN 0010-9312

Parkins, R. (1990). Strain rate effects in stress-corrosion cracking – 1990 Plenary Lecture, *Corrosion*, Volume 46, Issue 3 (Mar 1990), pp. 178-189, ISSN 0010-9312

Perdomo, J.; Morales, j.; Viloria, A. & Lusinchi, A. (2002). Carbon dioxide and hydrogen sulfide corrosion of API 5L grades B and X52 steels, *Materials Performs*, Volume 41, Issue 3 (Mar 2002), pp. 54-58, ISSN 0094-1492

Presage of production of the marine and south regions from México for a horizon of the 2000-2014

Shim, I. & Byrne, J. (1990). A study of hydrogen embrittlement in 4330 steel. 1. Mechanical aspects, *Materials science and engineering A*- Structural materials properties microstructure and processing, Volume 123, Issue 2 (Feb 1990), pp. 169-180, ISSN 0921-5093

Stress Corrosion Cracking on Canadian Oil and Gas Pipelines, (1996), Edited by National Energy Board (NEB), (December 1996), p. 16. ISBN 0-662-81679-X.

Takahashi, A. & Ogawa, H. (1995). Influence of softened heat-affected zone on stress oriented hydrogen-induced cracking of a high-strength line pipe steel, *ISIJ International*, Volume 35, Issue 10 ((1995), pp. 1190-1195, ISSN 0915-1559

Takahashi, A. & Ogawa, H. (1996). Influence of microhardness and inclusion on stress oriented hydrogen induced cracking of line pipe steels, *ISIJ International*, Volume 36, Issue 3 (1996), pp. 334-340, ISSN 0915-1559

Takahashi, A; Hara, T. & Ogawa, H. (1996). Comparison between full scale tests and small scale tests in evaluating the cracking susceptibility of line pipe in sour environment, *ISIJ International*, Volume 36, Issue 2 (1996), pp. 229-234, ISSN 0915-1559

Tsay, L.; Lin, Z.; Shiue, R. & Chen, C. (2000). Hydrogen embrittlement susceptibility of laser-hardened 4140 steel, *Materials science and engineering A-Structural materials properties microstructure and processing,* Volume 290, Issue 1-2 (Oct 2000), pp. 46-54, ISSN 0921-5093

Vangelder, K.; Erlings, J.; Damen, J. & Visser, A. (1987). The stress-corrosion cracking of duplex stainless-steel in $H_2S/CO_2/Cl^-$ environments, *Corrosion Science*, Volume 27, Issue 10-11 (1987), pp. 1271-1279, ISSN 0010-938X

Vega, O.; Hallen, J.; Villagomez, A. & Contreras, A. (2008). Effect of multiple repairs in girth welds of pipelines on the mechanical properties, *Materials Characterization,* Volume 59, Issue 10 (Oct 2008), pp. 1498-1507, ISSN 1044-5803

Vega, O.; Villagomez, A.; Hallen, J. & Contreras, A. (2009). Sulphide stress corrosion cracking of multiple welding repairs of girth welds in line pipe, *Corrosion Engineering, Science and Technology,* Volume 44, Issue 4 (Aug 2009), pp. 289-296, ISSN 1478-422X

Wang, S.; Chen, W.; King, F.; Jack, T. & Fessler, R. (2002). Precyclic-loading-induced stress corrosion cracking of pipeline steels in a near-neutral-pH soil environment, *Corrosion*, Volume 58, Issue 6 (Jun 2002), pp. 526-534, ISSN 0010-9312

Wang, S.; Zhang, Y. & Chen, W. (2001). Room temperature creep and strain-rate-dependent stress-strain behavior of pipeline steels, *Journal of Materials Science*, Volume 36, Issue 8 8Apr 2001), pp. 1931-1938, ISSN 0022-2461

Wilhelm, S. & Kane, R. (1984). Effect of heat-treatment and microstructure on the corrosion and SCC of duplex stainless-steels in H_2S/Cl^- environments, *Corrosion*, Volume 40, Issue 8 (1984), pp. 431-439, ISSN 0010-9312

Zhang, X.; Lambert, S.; Sutherby, R. & Plumtree, A. (1999). Transgranular stress corrosion cracking of X60 pipeline steel in simulated ground water, *Corrosion*, Volume 55, Issue 3 (Mar 1999), pp. 297-305, ISSN 0010-9312

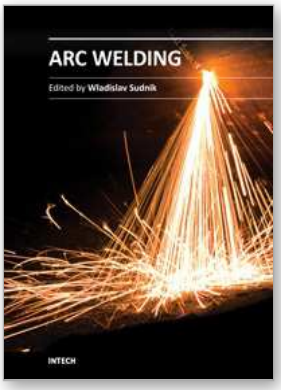

Arc Welding

Edited by Prof. Wladislav Sudnik

ISBN 978-953-307-642-3
Hard cover, 320 pages
Publisher InTech
Published online 16, December, 2011
Published in print edition December, 2011

Ever since the invention of arc technology in 1870s and its early use for welding lead during the manufacture of lead-acid batteries, advances in arc welding throughout the twentieth and twenty-first centuries have seen this form of processing applied to a range of industries and progress to become one of the most effective techniques in metals and alloys joining. The objective of this book is to introduce relatively established methodologies and techniques which have been studied, developed and applied in industries or researches. State-of-the-art development aimed at improving technologies will be presented covering topics such as weldability, technology, automation, modelling, and measurement. This book also seeks to provide effective solutions to various applications for engineers and researchers who are interested in arc material processing. This book is divided into 4 independent sections corresponding to recent advances in this field.

How to reference

In order to correctly reference this scholarly work, feel free to copy and paste the following:

A. Contreras, M. Salazar, A. Albiter, R. Galván and O. Vega (2011). Assessment of Stress Corrosion Cracking on Pipeline Steels Weldments Used in the Petroleum Industry by Slow Strain Rate Tests, Arc Welding, Prof. Wladislav Sudnik (Ed.), ISBN: 978-953-307-642-3, InTech, Available from: http://www.intechopen.com/books/arc-welding/assessment-of-stress-corrosion-cracking-on-pipeline-steels-weldments-used-in-the-petroleum-industry-

INTECH
open science | open minds

InTech Europe
University Campus STeP Ri
Slavka Krautzeka 83/A
51000 Rijeka, Croatia
Phone: +385 (51) 770 447
Fax: +385 (51) 686 166
www.intechopen.com

InTech China
Unit 405, Office Block, Hotel Equatorial Shanghai
No.65, Yan An Road (West), Shanghai, 200040, China
中国上海市延安西路65号上海国际贵都大饭店办公楼405单元
Phone: +86-21-62489820
Fax: +86-21-62489821